From Optical Ray Tracer Design to Lens Performance Analysis

Alan Liu

***Abstract*-In this experiment, I designed a 3-D ray tracer, achieving refraction and reflection of rays at arbitrary spherical and planar optical elements, by defining classes such as Ray and Optical-elements as well as methods like propagate. In the model validation stage, I mainly compare the RMS spot values for two lens configurations: plano-convex (PC) and convex-plano (CP) at different ray bundle sizes and quantitatively compared with the theoretical diffraction limits. The results show that the spherical aberration rapidly exceeds the diffraction limit after a radius of more than about 1.5 mm, and that the RMS of the CP configuration is always lower than that of the PC due to the geometrical advantages of the principal plane offset and curvature distribution.**

I. INTRODUCTION

This experiment aims to design a generalized 3-D ray tracer model which is coincidence with physical principles and then use it to analyze the paths of the rays and quantitatively determine the spherical aberration of those different lenses. The most important formula in this experiment is Snell's Law, which can be expressed as:

$$n_1 sin\theta_1 = n_2 sin\theta_2 \quad (1)$$

where n_1 and n_2 are refraction indexes of different materials, θ_1 and θ_2 are the incident and refraction angle respectively. Refraction or total internal reflection when passing through any optical element must follow this law. [1]

II. METHODOLOGY

A) Experimental set up

To implement the full functionality of the ray-tracer, I organize the code into several key classes. First, the Ray class represents a single light ray by storing its current 3D position and propagation direction; its append method records each new vertex whenever the ray changes direction. To handle many rays simultaneously, I use the Ray Bundle class, which generates a set of rays on concentric rings and makes them iterable for per-ray processing.

Next, the General-Surface class with its subclasses Spherical-Refraction, Spherical-Reflection and Output Plane can model all optical elements. Each surface is defined by three primary parameters: z_0: the z-axis coordinate of the vertex; aperture: its clear semi-diameter, and curvature (1/R): zero for a plane, nonzero for a sphere of radius R. A core method in this class is intercept, which solves the ray–surface intersection (either the plane intersection $z=z_0$ or the quadratic intersection with a sphere of radius R), returning the 3D point Q or None if there is no valid hit. In The spherical-surface case, intersection is obtained by solving a quadratic equation:

$$\left|r + l\hat{k}\right|^2 = R^2 \quad (2)$$

Where r is the vector from the sphere's center to the ray's starting point and $\hat{k}$ is the unit vector in the direction of the ray. l is the distance between the starting point and the intersection [1]. If the discriminant is negative, there is no real intercept, and we discard that ray. If there are two positive roots, we select the physically correct intersection point, choosing the nearer root for curvature < 0 case and the farther root for curvature > 0 case. Another crucial method is called propagate, which manages the passage of a ray through a set of surfaces. After obtaining the intersections and current directions, it will automatically calculate the new direction according to Snell's Law and updates the Ray object with the new vertex and direction.

Finally, the Plano-convex and Biconvex classes each build a lens by instantiating two Spherical-Refraction surfaces (with the appropriate curvatures, refractive indices, and spacing). Each lens class also provides a focal point method: for plano-convex lens cases I use the standard lens maker's formula as rays will not refract passing through the first plane, but for convex-plano lens I adds an extra correction term that accounts for the principal-plane shift introduced by the finite center thickness. The lens maker's formula and the correction are expressed in equation 3 and 4 respectively. [2]

$$\frac{1}{f} = (n-1) * \left(C_1 - C_2 + \frac{(n-1) * d * C_1 * C_2}{n}\right) \quad (3)$$

$$H = \frac{(n-1) * d * C_1}{n * (C_1 - C_2)} \quad (4)$$

Where f is the focal length, n is the refractive index of the lens, C_1 and C_2 are the curvatures of the first and the second surface, d is the thickness of the length and H is the correction.

B) Data collection

During data collection, we first instantiate a ray bundle (with default values) and create the desired optical elements such as Spherical-Refraction surfaces and Output Plane. We then call each element's propagate method in sequence, passing each Ray through every surface and updating its position and direction via append method.

There are mainly three kinds of outputs, and firstly, 3D Track Plot: a three-dimensional rendering of each ray's trajectory through space, showing how rays refract or reflect off each surface. Secondly, Spot Plot, which is a two-dimensional scatter plot of the (x,y) coordinates of all rays in

the bundle at their current intercept plane (typically the focal plane), visualizing the focal spot distribution. And finally, numerical values are also important such as the focal length f of a lens, computed via the lens maker's or thick-lens formula and the RMS spot size of the ray bundle, which quantitatively determines the spherical aberration. It is defined as:

$$RMS = \sqrt{\frac{1}{N}\sum_{i=1}^{N}(x_i{}^2 + y_i{}^2)} \quad (5)$$

where (x_i,y_i) are the ray intercept coordinates in the focal plane and N is the total number of rays in the bundle. RMS is compared with the diffraction scale of the lens, which can be expressed as:

$$\Delta x = \frac{\lambda f}{D} \quad (6)$$

Where Δx is the diffraction scale, λ is the wavelength of incident light, f is the focal length and D is the aperture [1]. If RMS is less than or equal to Δx, the quality of image is mainly affected by diffraction, instead of the spherical aberration. Together, these visual and numerical outputs allow us to both qualitatively inspect ray paths and quantitatively evaluate lens performance and spherical aberration.

III. RESULTS & DISCUSSION

During my experiment process, I made a couple of key assumptions. First of all, I assume that the incident light is all monochromatic light with a wavelength of 588nm, ignoring the bandwidth and dispersion of the spectrum. In this case, I would not need to include a chromatic aberration correction element in the design. Secondly, since all the light rays are parallel to the main optical axis in the simulation, I ignore the higher-order nonlinearities of refraction and reflection, and do not add corrections for fringe rays. In addition, I also took into account the Fresnel Reflection Loss [3], and when trying to quantify this effect, I used this equation:

$$R = \left(\frac{n_1 - n_2}{n_1 + n_2}\right)^2 \quad (7)$$

Where R is the radio of reflection power to the incident power when normal incidence, n_1 and n_2 are the refractive index of air and glass respectively. I found that only about 4% of the total power of the incident light would be reflected back and the radio is lower when incident angle is not 90 degrees, so I chose to ignore this small factor.

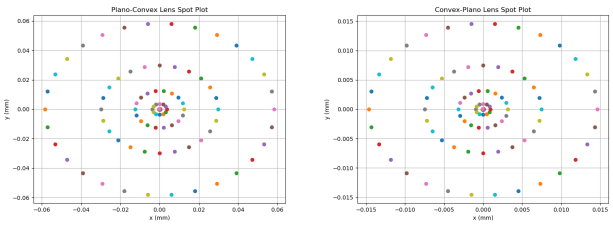

Fig 1: The spot plots at the paraxial focal point for PC lens (left) and CP lens (right) with default lenses parameters and default ray bundle.

By analyzing the above two graphs and data, I found that in the focal plane, the RMS value of Plano-Convex (PC) lens is 0.0372, while that of Convex-Plano (CP) lens is 0.00934, and the diffraction limit is 0.00569. It is obvious that the spherical aberration of the lenses is the main reason why the light beams cannot converge at one point.

Spherical aberration refers to the fact that the spherical surface cannot converge all incident parallel or near-axis light rays to the same point as an ideal paraboloid surface. This results in a blurring of the image on the output plane, the ideal dot is pulled into a speck, and the light rays in the center and at the edges do not coincide. In this experiment, the incident light is parallel to the optical axis, and the light rays at different heights focus on different positions, resulting in both longitudinal and transverse spherical aberration. Interestingly, the central symmetry of the initial ray bundle leads to numerical consistency in the final transverse and longitudinal spherical aberration.

In subsequent analysis I found that as the radius of the ray bundle gradually increases, the RMS of both lenses will rise and the diffraction limit will decrease, but the RMS of the CP lens is always smaller than that of PC lens. This is because when using the CP lens configuration, the light is converged once as it passes through the first plane, bringing the edge rays closer to the main optical axis, thus reducing spherical aberration after the second refraction. In addition, in thick lens theory [1], the principal plane of the lens might be shifted by the order of curvature. The principal plane of the CP lens is closer to the light source, resulting in a shorter back focal length from the principal plane to the focal point, and the fringing rays experience less accumulation of spherical aberration during the focusing process. While in the case of the PC lens, the principal plane is shifted to the other side, and the fringing light has to travel a longer distance before converging, thus accumulating more aberration.

To verify the correctness of the results, I also calculated the Seidel aberration coefficients [4] for the two lenses, and again, the results are that the value of CP lens is smaller than that of PC lens. In the subsequent analysis of the optimized biconvex lens with its RMS value of 0.00443, which is smaller than that of the CP lens, thus further demonstrating the result.

IV. CONCLUSION

In this experiment, I successfully developed a generalized 3-D ray-tracer and applied it to the quantitative analysis and optimization of simple spherical optics. Considering the track plots I got, the tracer correctly reproduces both refractive and reflective behavior on planar and spherical surfaces. And for the PC versus CP lens of the same glass and geometry, I showed through RMS spot-size vs. beam-radius curves that spherical aberration overtakes diffraction beyond 1.5 mm and that the CP orientation consistently yields smaller spot sizes. With the default ray bundle, RMS values at the focal plane for CP and PC lens are 0.00934 and 0.0372 respectively.

To further improve the existing model, I plan to introduce some chromatic aberration correction elements or add wavelength dependent refractive index in the design to deal with lights with different wavelengths. In addition, I will try to use unparallel rays and elements in other shapes to test the behavior and calculate the new RMS values. By addressing these extensions, the new ray tracer can evolve into a comprehensive optical design and analysis tool which is capable of handling complex, multi-element, broadband imaging systems.

REFERENCES

[1] Year 2 Lab Script: Computing project A, Imperial college London, 2024
[2] Hecht, Eugene (2017). "Chapter 6.1 Thick Lenses and Lens Systems". Optics (5th ed.). Pearson. ISBN 978-1-292-09693-3.
[3] Born & Wolf, 1970, p.40, eqs. (20),(21).
[4] Lin Zhi-Li (2007), "Seidel aberration of left-handed media lens systems", Acta Phys. Sin.

APPENDIX

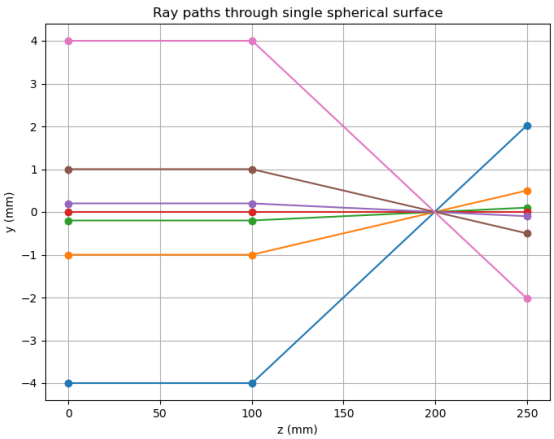

Fig 1: Track plot of the trajectory of example rays through a spherical surface at z_0 = 100mm with curvature 0.03mm^{-1}, aperture 34mm and refractive indices n_1 = 1.0 and n_2 = 1.5 and an output plane at z_0 = 250mm.

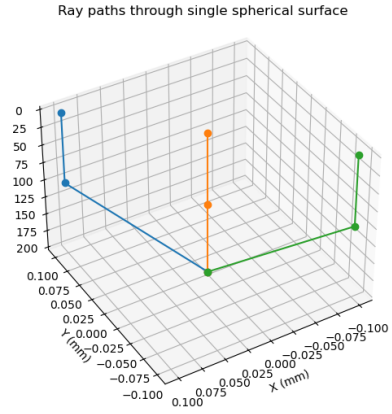

Fig 2: Track plot of the trajectory of paraxial rays through the same spherical surface.

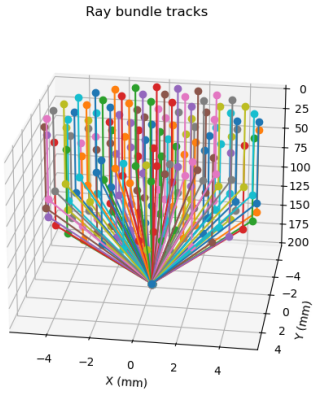

Fig 3: Tracing a 5mm diameter uniform bundle of collimated rays through the same specified spherical surface.

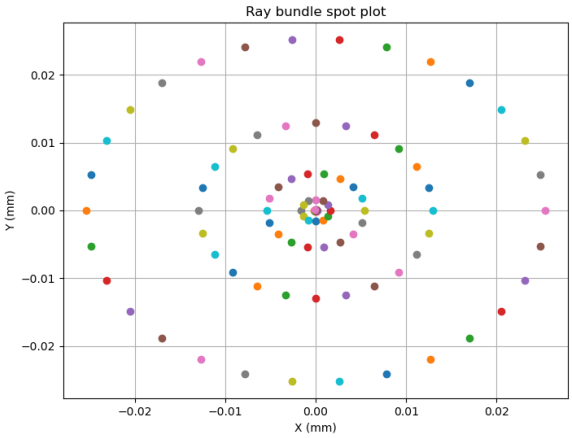

Fig 4: Corresponding spot diagram for the 5mm bundle of rays, at the paraxial focal plane.

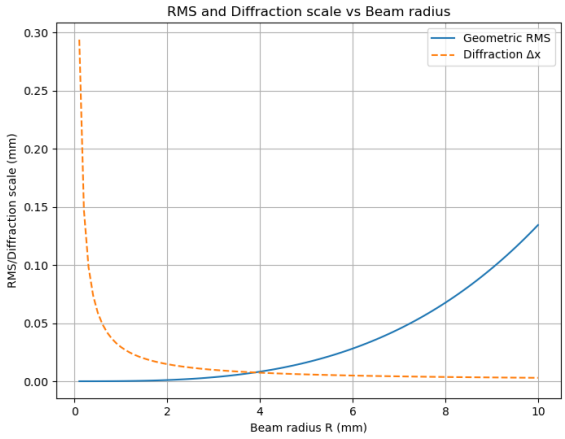

Fig 5: Plot showing how the RMS value compares to the diffraction scale.

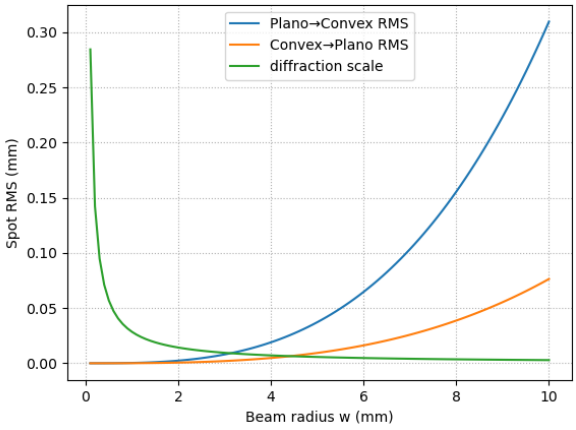

Fig 8: Plot comparing the RMS values of lenses in each orientation to the diffraction scale.

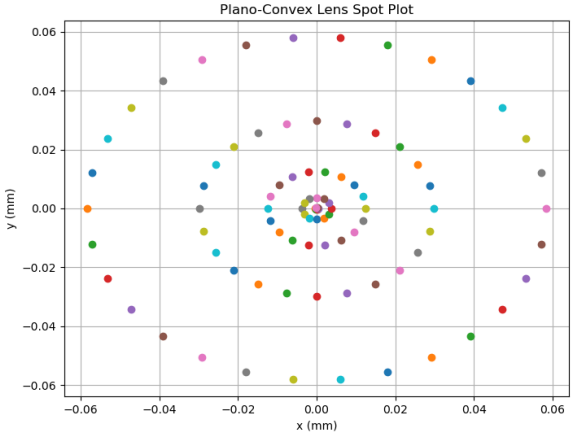

Fig 6: The spot plot at the paraxial focal point for PC lens with default lenses parameters and default ray bundle.

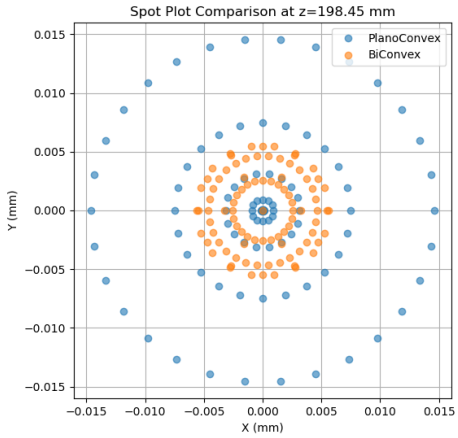

Fig 9: Combined spot plot from the Plano-convex and optimized Biconvex lenses with lowest RMS value at the focal point of PC lens.

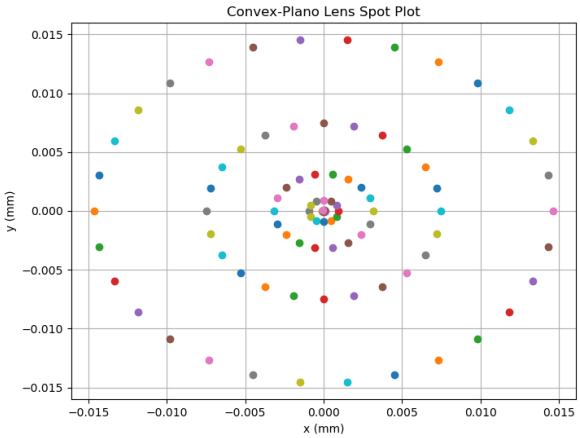

Fig 7: The spot plots at the paraxial focal point for CP lens with default lenses parameters and default ray bundle.

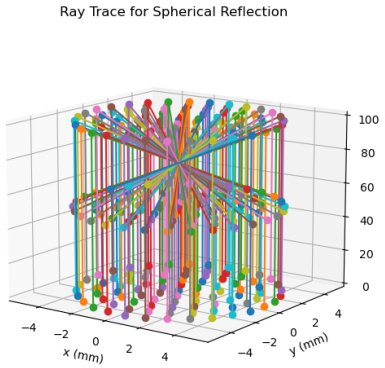

Fig 10: Track plot for the Spherical Reflection surface with z_0=100mm, aperture=6mm, curvature=-0.02, output surface at z_0=50mm and a default ray bundle.